Alternative Optical Technologies - More than curiosities?

Bruce W. Smith
Rochester Institute of Technology, Microsystems Engineering
77 Lomb Memorial Dr., Rochester, New York 14624, bwsemc@rit.edu

ABSTRACT

As optical lithography reaches it physical limits, alternative technologies become interesting. There have been several such alternatives that are still optical, but have some departure from conventional projection methods. This papers presents some of these alternative optical technologies, namely the use of surface plasmons and plasmonic lithography, metamaterials and superlenses, evanescent wave lithography, solid immersion lithography, and stimulated transmission depletion (StED) lithography. Additionally, the viability of interferometric lithography (IL) is addressed for application to sub-32nm generations by using an information content metric and comparing results to 193nm lithography, double patterning, and EUV.

Keywords: Nanolithography, plasmonic lithography, metamaterials, superlenses, evanescent wave lithography, solid immersion lithography, StED lithography, interferometric lithography

1. INTRODUCTION

As the limits of “conventional” optical lithography are being reached, possibilities of extension using technologies that are less mainstream may become intriguing. To begin with, the meaning of *conventional optical lithography* needs to be clarified. Approaches which were once considered enhancements to optical lithography have become prevalent in most semiconductor manufacturing. Whether it is phase-shift masking, customized illumination, optical proximity correction, polarized imaging, or immersion lithography, the lithographer has come to depend on these options to achieve sub-wavelength resolution. In hindsight, the insertion of such resolution enhancement techniques has been the implementation of fairly well understood optical phenomena that are more commonplace in other optics fields, such as those described by Reynolds [1]. The meaning of the *limits* of optical lithography also needs to addressed. Although the demise of optical lithography has been predicted or projected for several decades, it isn’t until the physics makes imaging impossible that we reach true limits. The diffraction limits for projection lithography dictate that it is not possible to image a geometry with a pitch value smaller than $\lambda/(2n)$, where n is the refractive index of the image media. It has been the ingenuity of the lithographer that has allowed for manufacturable resolution to reach these limits.

The true limits of optical lithography are therefore upon us. With the ArF excimer wavelength of 193nm as the shortest UV optical lithography wavelength and the refractive index of water (1.44) as the highest media index, optical lithography cannot deliver geometry beyond a 33.5nm half pitch. Rebalancing of line-to-space duty ratio can allow for smaller linewidth geometry but without additional process tricks (such as the use of a sidewall spacer double patterning process) or multiple pass process-exposure steps, a pitch below 67nm cannot be attained. This paper will not address approaches to double patterning, nor will it address whether materials could be employed with higher refractive indices. Instead, a number of non-mainstream technologies will be explored that have been getting some recent attention. This paper presents an overview of some of these technologies in the perspective of what we may consider mainstream, namely high NA projection lithography.

2. ALTERNATIVE OPTICAL TECHNOLOGIES

A list of alternative optical techniques may include high index immersion, double patterning, maskless lithography, and self-assembly, which have been discussed in great detail in the lithography community. Topics that have not been paid much attention in the lithography field but have gained interest in other areas of nanotechnology include surface plasmons and plasmonic lithography, metamaterials and superlenses, evanescent wave lithography, solid immersion lithography, stimulated transmission depletion (StED) lithography, and interferometric lithography. The question posed by the lithography is whether these technologies are viable for manufacturing or merely useful for research and development applications.

Optical Microlithography XXII, edited by Harry J. Levinson, Mircea V. Dusa, Proc. of SPIE Vol. 7274,
727402 · © 2009 SPIE · CCC code: 0277-786X/09/$18 · doi: 10.1117/12.817219

Downloaded from SPIE Digital Library on 27 Jan 2010 to 129.21.240.32. Terms of Use: http://spiedl.org/terms

2.1 Surface Plasmons and Plasmonics

Compared to optics (or photonics) where light is controlled by dielectric materials, plasmonics is where light is controlled by metal structures through surface plasmons. Surface plasmons are propagating free electron oscillations bound to the interface between a dielectric and a metal. They are not subject to classical diffraction limits but they couple strongly to light, forming surface plasmon polaritons (SPPs).

The simplest way to excite surface plasmons is coat a very thin (20-50nm) metal film onto the base of a prism, as shown in Figure 1. Aluminum or silver suffice as metal films for visible wavelengths. The particular requirements of such a film will be addressed later. If we illuminate a face of the prism with monochromatic UV-visible TM polarized light at angles beyond total internal reflection (TIR), light is reflected out of the opposite prism face. By carefully tuning the incident angle beyond TIR, a resonance angle is reached, where the frequency and wavelength of the light impinging on the metal surface matches the resonance of surface plasmons. There is a decrease in reflection and a very bright transmission spot at the metal-air interface. SPs are excited and the evanescent field penetrates the thin metal film. This is plotted in Figure 2 from a classical experiment by Martini [2]. Here, the Y-axis represents the transmission at the metal-air interface, where the light exiting the film at the resonance angle is brighter than what would be predicted based on the penetration depth of the metal film.

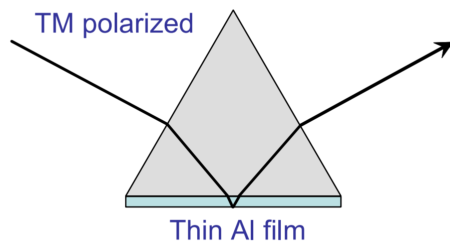

Figure 1. (above) A prism method to generate surface plasmons, where TM light enters the prism to excite SPs at the metal-dielectric interface at the critical resonance angle.

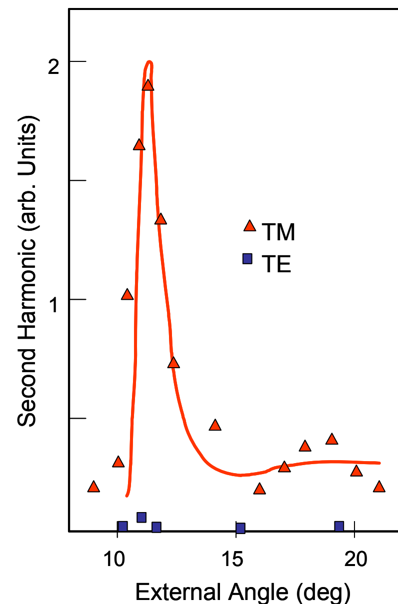

Figure 2. (right) Enhancement of surface plasmons at the metal-dielectric interface, plotted as the second harmonic generation (transmission at the prism base) verses resonance angle.

Surface plasmons can therefore be thought of as a traveling charge density or propagating electron oscillations on the surface of a metal. Figure 3 shows the SP wave traveling on the surface of a metal, with its amplitude extending further into the dielectric region. The electric field oscillates in the incident plane, or in the plane of the page, correlating to the coupling effect that occurs only with TM polarization.

The potential of SPs is interesting due to their sub-wavelength nature. The dispersion curve of Figure 4 shows how the wavelength of excited surface plasmons is shorter than the exciting photon wavelength at the same frequency, determined by the electrical and optical properties of the metal and its surrounding, where k_0 is the wave vector in vacuum and k_{sp} is frequency dependent SP wave vector. Generally, light can't directly excite SPs unless the momentum of SPs and the light waves are matched. This matching can be achieved through reflection, as described above, or by using surface structure such as gratings, holes, or roughness.

Downloaded from SPIE Digital Library on 27 Jan 2010 to 129.21.240.32. Terms of Use: http://spiedl.org/terms

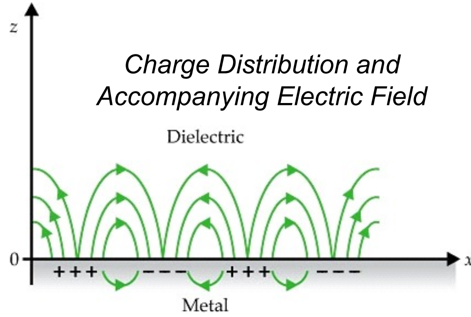

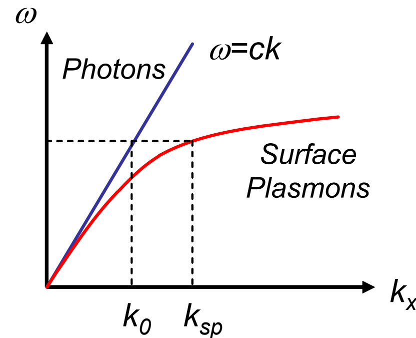

Figure 3. A surface plasmon can be thought of as a traveling charge density on the surface of a metal.

Figure 4. A plot showing how the wavelength of excited surface plasmons is shorter than the exciting photon wavelength at the same frequency. k_0 is the wave vector in vacuum and k_{sp} is frequency dependent SP wave vector

2.2 Plasmonic Lithography

So how could the phenomena of surface plasmons be used for lithography? A plasmonic lithography approach has been introduced to image sub-wavelength nano holes [3]. Geometric optics predicts that the transmission through a very small hole falls off rapidly with radius as r/λ^4. As shown in Figure 5, a nanohole array mask is made up of a 80nm Al film surrounded by dielectric materials such as a quartz substrate and a PMMA spacer layer with matched refractive indices. The holes in the array are 90nm on a 170nm pitch (below lambda/2 for 365nm wavelength). Surface plasmons can be excited in such a mask by tuning sizing, wavelength, and materials so that the permittivity of the metal surrounded by the dielectric is negative Surface plasmons then tunnel through the holes, scatter at the bottom, and re-propagate into a photoresist coated beneath the spacer layer. There can be an almost 10X enhancement in transmission from the plasmonic resonance effect compared to that for a single hole, leading to an exposure similar to what would be expected for a far-field imaging. The inherent problems of this approach can be related to it being a near-field technology, the availability of materials, and how this scales to shorter wavelengths. Hole sizes here are $\lambda/4$. If it could be scaled to 193nm, the holes size would be 48nm on a 90nm pitch.

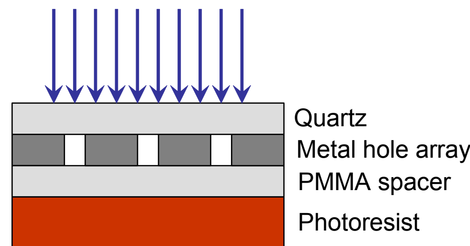

Figure 5. A plasmonic mask using a quartz substrate, a thin metal hole array, and a polymeric spacer. UV-visible radiation is directed onto the mask and holes are imaged into a photoresist film.

An extension to plasmonic lithography has been presented using silver plasmonic lenses with concentric rings to concentrate light to a hole in the center, where it exits on the other side [4]. In this approach, the hole is 80nm in diameter and 100,000 parallel lenses could be packed into a flying plasmonic head for maskless lithography, possibly for patterned magnetic media applications. The head would "fly" above the photoresist surface at speeds up to 12 m/s with a 20nm gap. If the 80nm holes at a 365nm wavelength were scaled to the 193nm ArF excimer laser wavelength, the resulting hole size would be 42nm and the required gap would be reduced to 5-10 nm, and possible less. Also, if scaled to 193nm, silver is no longer a viable candidate for the generation of surface plasmons.

Downloaded from SPIE Digital Library on 27 Jan 2010 to 129.21.240.32. Terms of Use: http://spiedl.org/terms

2.3. Solid Immersion Lithography

A few years ago, the idea of adapting the solid immersion lens (SIL) was introduced to lithography and referred to as solid immersion lithography [5]. The name is a bit confusing because with SIL, a small air gap remains between the lens and the substrate. The evanescent field at the lens-air interface jumps across the sub-100nm gap to be frustrated by and re-propagate into a higher index media. The exponential decay is rapid, depending on the material indices and angles involved, but sufficient transmission may be achieved.

$$A(z) = e^{-\left(\frac{2\pi n_{upper}}{\lambda}\left[\sin^2\theta - \left(\frac{n_{lower}}{n_{upper}}\right)^2\right]^{1/2} + \alpha\right)z}$$

Figure 6 shows a plot of the gap requirements for solid immersion lithography using a water gap instead of an air gap, referred to as solid-liquid immersion lithography (SLIL). For 28nm half pitch at 1.72 NA (in sapphire), a gap of 30nm is tolerable to produce 50% transmission in photoresist. A higher refractive index fluid may allow for a gap near 100nm. The resolution here is nearly λ/7, compared to the λ/4 of the plasmonic lithography approach.

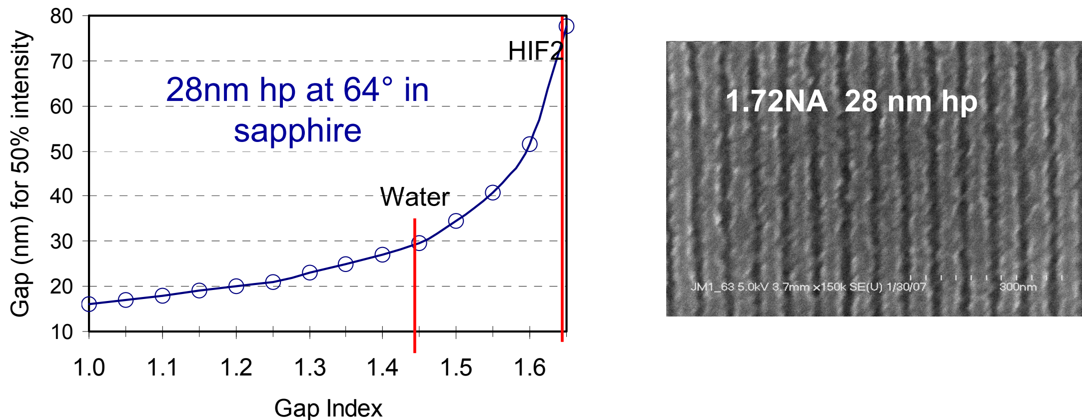

Figure 6. A plot of the gap requirement for solid-liquid immersion lithography as the gap is index is increased from 1.0 (air). The SEM photograph on the right is of 28nm half-pitch lines in photoresist images with a high refractive index fluid.

2.4 Evanescent Wave Lithography

The concept of evanescence and evanescent waves is closely related to surface plasmonic effects. As described above, evanescent waves do not propagate unless somehow frustrated, such as with a higher index medium. An evanescent field can be generated several ways, including total internal reflection, the scattering from a small aperture, and the diffraction from a grating. The diffracted field of a zero-order grating includes surface bound evanescent energy as a collection of the evanescent waves emanating from each aperture. Lezec showed how an opening in a metal film over glass surrounded by periodic grooves creates evanescent waves which form a composite diffracted evanescent wave (CDEW) traveling toward the opening and increasing transmission [6]. We have expanded these concepts for application to a photomask and describe the enhancement using Evanescent Wave Assist features (EWAF). We recently showed how sub-diffraction grooves pattered between a mask substrate and an absorber can produce CDEWS to enhance the transmission of a photomask opening, which can propagate to the far field and result in improved image contrast [7], as depicted in Figure 7.

Downloaded from SPIE Digital Library on 27 Jan 2010 to 129.21.240.32. Terms of Use: http://spiedl.org/terms

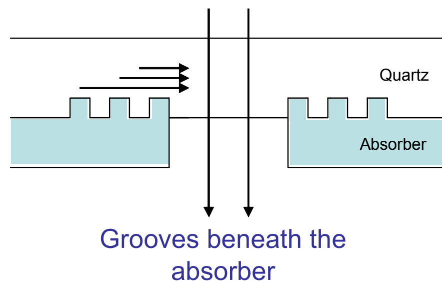

Figure 7. A schematic of a photomask employing evanescent wave assist features (EWAF) between the mask substrate and the absorber.

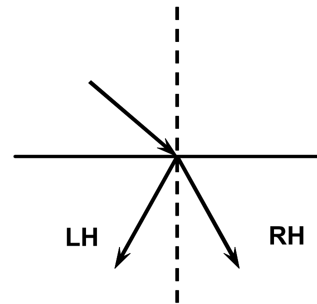

Figure 8. A depiction refraction from normal (right-handed) materials and left-handed materials, also known as metamaterials.

2.5 Metamaterials and a Sub-Diffraction Superlens

Negative refractive index materials are also known as metamaterials. Such a material could reverse conventional optical phenomena, as shown in Figure 8. For negative refractive index, both the permittivity (ε) and the permeability (μ) of the material need to be less than zero. Because electromagnetic effects decouple at sub-wavelength scales, the requirement for TM polarized light is that only the permittivity has to be negative. This can be achieved with Al and Ag at UV-visible wavelengths.

A thin metamaterial can then act as a superlens to converge diffracted rays and image beyond diffraction limits [8]. The decaying wave can increase exponentially as it propagates into and through a planar metamaterial lens. On the other side of the superlens, the field decays again until it has reached its original value at the image plane. The superlens then acts as an intimate contact mask to recover decaying evanescent waves. Using silver as a natural optical superlens, Fang and co-workers demonstrated sub–diffraction-limited imaging with 60 nm half-pitch resolution, or one-sixth of the illumination wavelength.

2.6 Metamaterials for 193nm

As applications for metamaterials or superlenses for 193nm lithography are explored, at least two questions need to be addressed. Namely, are there suitable choices for metamaterials at 193nm and if so what application would it have for projection lithography? It is difficult to envision an imaging approach using a superlens as the primary mechanism to image real device geometry. It may be possible, however, to use some of the image enchantment concepts enabled by metamaterials in some aspect of a lithography system

A first requirement that should be established is that the basic configuration of a superlens "stack" will be a thin metal film surrounded by a dielectric. This may allow for candidate materials that could meet the requirement of negative permittivity (for TM polarized radiation). Figure 9 is a plot of the refractive index vs. extinction coefficient of aluminum and aluminum oxide (Al_2O_3) along with curves showing solutions for the matching of the magnitude of the permittivity of a material to that of the surrounding dielectric, while driving the value negative as n^2-k^2. Suitable metamaterials fall at the intersection of these curves. Neither aluminum or stoichiometric aluminum oxide fall near these intersections but composites of the two may. By adjusting the nanostructure of such composites, and the corresponding depolarization factor (q), solutions are possible.

Downloaded from SPIE Digital Library on 27 Jan 2010 to 129.21.240.32. Terms of Use: http://spiedl.org/terms

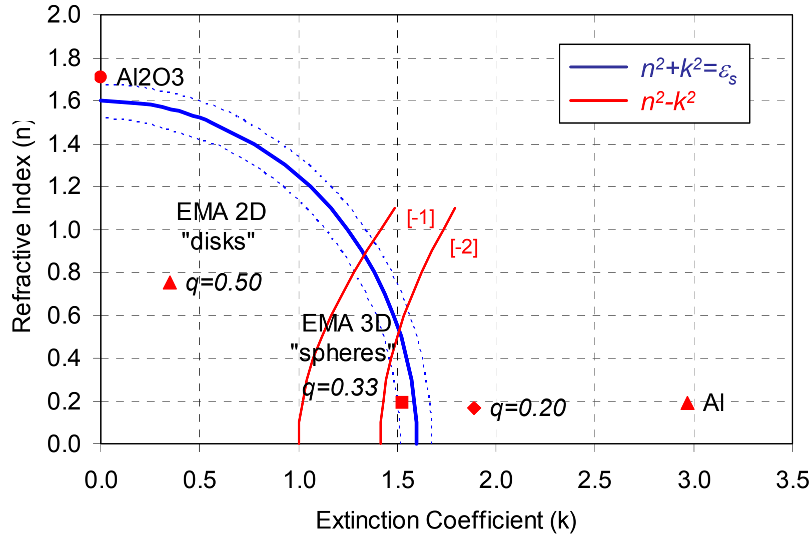

Figure 9. A plot of the optical properties of aluminum, aluminum oxide, and composites along with the requirements for negative permittivity behavior when sandwiched between a dielectric film with a refractive index near 1.70.

One application of a metamaterial for 193nm lithography is the near field lithography condition created using a contact enhancement layer (CEL). Through the use of a slowly bleaching film coated over a photoresist, the concept of contrast enhancement has existed in lithography for many years [9]. There has been a renewed interest in such materials lately as double patterning is pursued for sub-diffraction limited resolution. The use of a metamaterial beneath such a CEL and above an index matched spacer layer can allow for the creation of an evanescent wave superlens (EW-CEL) and shown in Figure 10. Figure 11 shows the simulated intensity image for a 30nm space opening above and below a 20nm Al-O composite film, coated under a 50nm CEL.

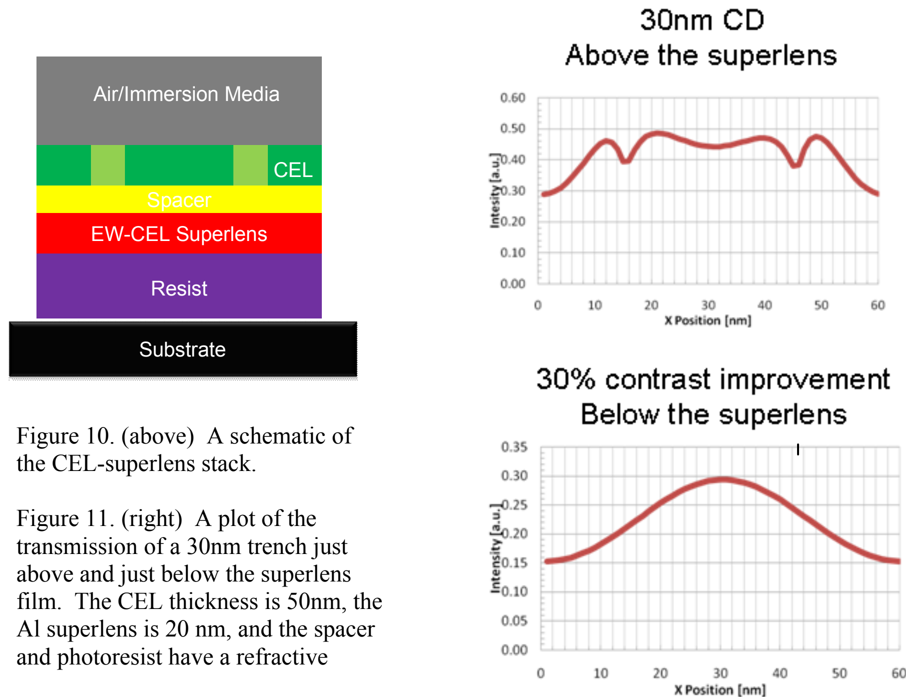

Figure 10. (above) A schematic of the CEL-superlens stack.

Figure 11. (right) A plot of the transmission of a 30nm trench just above and just below the superlens film. The CEL thickness is 50nm, the Al superlens is 20 nm, and the spacer and photoresist have a refractive

Downloaded from SPIE Digital Library on 27 Jan 2010 to 129.21.240.32. Terms of Use: http://spiedl.org/terms

A second application for a 193nm superlens stack is a high-pass pupil filter (HPPF) , as shown in Figure 12. In high NA projection lithography a filter allowing selective polarized radiation at oblique angles is desired, while rejecting DC components and polarized radiation of the opposite state. An example pupil filter is comprised of infinitely thick silicon dioxide film (n = 1.55, k = 0) as the outer dielectric layer, a material with n = 2.4, k = 0 and varying thickness as the inner dielectric, and 13 nm thick aluminum metamaterial. A TE pass filter can be achieved when the closest dielectric (M2) has a higher permittivity than the farther dielectric (M1). On the other hand, a TM pass filter results as M2 has a lower permittivity than M1. Figure 13 shows transmission through the stack for TE and TM polarized 193 nm radiation, while varying both the inner dielectric thickness and the angle of incidence. An inner dielectric thickness of 73 nm provides nearly 100% TE transmission for angles near 80-85°. TM transmission over this same range of angles falls from 20% to near zero. The transmission for both polarization states is near equal at angles below 60°.

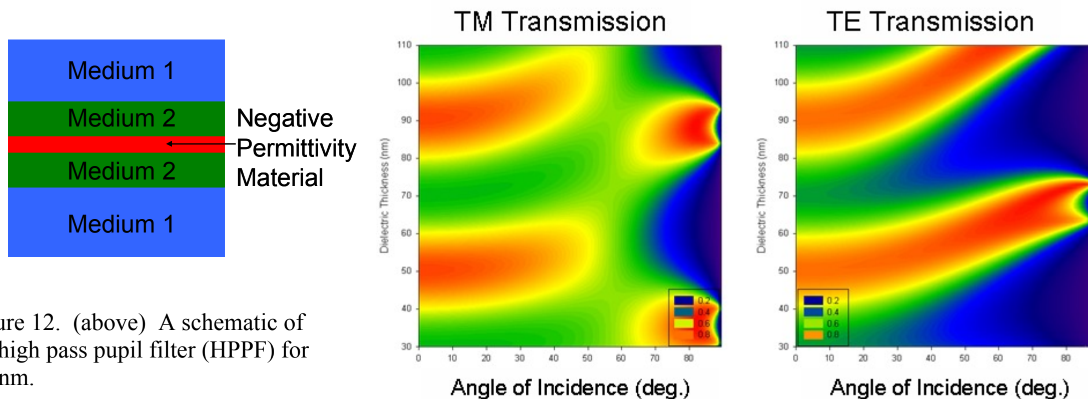

Figure 12. (above) A schematic of the high pass pupil filter (HPPF) for 193nm.

Figure 13. (right) A plot of the TE and TM transmission for the HPPF.

2.7 Stimulated Emission Depletion Lithography

Stimulated Emission Depletion (StED) is a phenomena that uses the non-linear de-excitation of fluorescent dyes to overcome the limits of diffraction [10]. StED microscopy reduces the diffraction region of a very short excitation pulse by following it with a "depletion" ring or doughnut pulse, tuned to an emission line of the fluorescent dye. This depletion pulse causes stimulated emission, moving electrons from the excited state (from which fluorescence occurs) to a lower energy state. The center of the doughnut is zero, causing a sharp trim around the axis of the excitation pulse field. After both pulses have been sent, fluorescence from the remaining excited dye molecules can be detected by the microscope with 12X improvement in resolution [11]. Extending StED concepts to lithography requires other photoinducable transitions, such as ground/excited states, molecular conformational states, photochromic states, or binding and protonation states [12]. By initiating a photo-inducible reaction from an initial state (A) to a state of temporary storage (B), together with a pathway for a spontaneous B to A transition, externally triggering using light, heat, or a chemical reaction can lead to a non-linear reversible imaging process. By combining this with a masking function that is shifted along a x-direction in small increments δx, sub-resolution patterning could be made possible. The challenges with such a process is the identification of materials that could possess the required properties. The challenge becomes more difficult with decreasing wavelength.

3.0 INTERFEROMETRIC LITHOGRAPHY

Interferometric lithography (IL) has been utilized for nanopatterning for several years and is responsible for some of the highest resolution 193nm immersion lithography, as shown in Figure 14 [13]. IL has been explored for template-based lithography using combinations of phase-shift masking (PSM), where two-beam interference is carried out in projection optics combined with a second masking step and standardized and reusable PSM templates [14]. With the regular structure of the logic type cells, patterns that are restricted at fundamental spatial frequencies could be created

Downloaded from SPIE Digital Library on 27 Jan 2010 to 129.21.240.32. Terms of Use: http://spiedl.org/terms

using two-beam interference. Whether this fundamental frequency is 1X the cutoff frequency of the projection system or 2X the frequency, where double patterning would not be necessary, it becomes evident that most of the frequency space of the projection lens pupil would not be utilized for such exposures. IL is therefore an approach that is well suited for this type of imaging. Figure 15 shows how logic type patterning can be designed for IL on a Cartesian grid to greatly simplify device patterning and allow the tightening of design rules, compared to more arbitrary layout. By printing regular gratings using IL on either a single axis or on X/Y axes (as shown) and following each with a separate trim step using either projection lithography (PL) or ebeam lithography (EBL) exposure, cell patterning can be achieved. The bulk of the patterning is carried out at a single frequency, limiting the information capacity requirement in the patterning step. If the trim exposure steps can be carried out at a lower spatial frequency, the trim system can be one or more generations lower (N-1, N-2, etc.) than what would otherwise be necessary for patterning using PL alone. Lithography challenges are not limited to resolution or CD control alone, however, and overlay requirements must also be met. Sufficient control over the registration between the template IL and trim steps must be met, as well as tight control over the overlay between the individual masking layers which are now decomposed into two separate imaging methods. If the high spatial frequency patterns are limited to one direction only, the sequence of Figure 15 is of course simplified, requiring just a single template IL exposure step followed by one trim step. The optical independence of the X and Y template IL exposures allow for additional frequency content at intersections, which may be beneficial or not, depending on the tolerable level of pattern proximity effects.

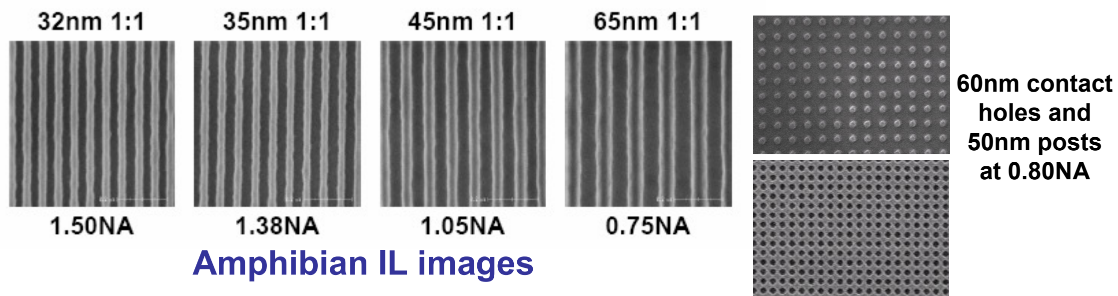

Figure 14. SEM photographs of images in resist created with 193nm immersion interferometric lithography at numerical apertures between 0.75 and 1.50.

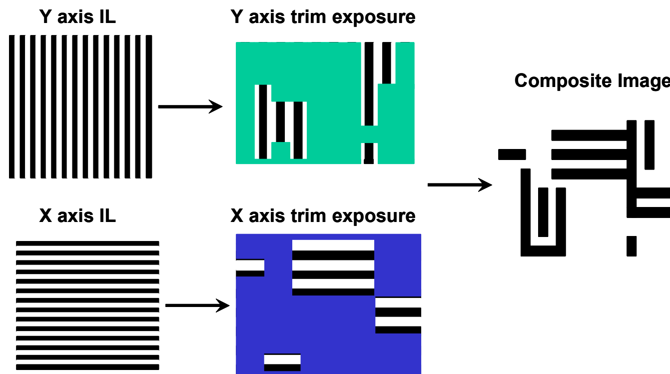

Figure 15. A depiction of a lithography process using two stages of interferometric imaging (IL) imaging and two stages of projection lithography (PL) trim.

A key problem associated with the analysis of current lithography options is the failure to evaluate technologies based on the information content that is processed and the cost of that processing. For example, if a conventional optical lithography projection system is considered, the information content (I) is the number of picture elements (or bits) processed by the system. This can be calculated by knowing the projection lens numerical aperture (NA), field size, wavelength, and the efficiency function (k_1 factor). This unitless figure of merit is useful for comparison of various systems:

$$I = \frac{field\ radius \times NA}{4k_1\lambda}$$

Downloaded from SPIE Digital Library on 27 Jan 2010 to 129.21.240.32. Terms of Use: http://spiedl.org/terms

This metric is a variation of the concept of the optical invariant that is used when evaluating optical system designs. For a dry 193nm lithography scanner operating at 0.9NA with a field size of 26mm, assuming a k-factor of 0.4, the amount of data that can be processed equates to 4.6×10^4 bits. If the resist exposure time is estimated at 0.1 sec, the data rate of the system is on the order of 4.6×10^5 bits/sec. There is no assumption regarding the structure of the image or the filtering of the image structure. In fact, if the image structure is frequency filtered, such as with off-axis illumination, phase shift masking, or the like, the data rate is not proportionally increased but may instead be decreased (due to losses in transmitted energy). When a design is considered so that only select frequencies are utilized or exist on the mask, the frequencies that are not populated remain available in the projection lens pupil, which is essentially wasted capacity. As an example, if a DRAM cell masking layer for a wordline line-space grating is considered, where over 70% of the design might be regular structure, the majority of the projection lens field is not used. The actual amount of data processed and the data rate of the lens are a small fraction of its capacity. As the relative amount of repetitive structure is increased, the processed data decreases. A lithography option which matches the required device patterning data rate to systems capability would be a more cost and time effective solution than one which could accommodate any arbitrary data type. Manufactures of lithography systems have been reluctant to develop systems for specific patterning applications, leading to optical projection and EUV tools which need to address all needs. The economics of more specialized systems could make sense, however, if tool cost can be made substantially lower. Interferometric lithography systems may provide such an option, meeting both the data processing needs and the lower cost option to alternatives. An additional incentive may be that IL can achieve what is not possible, namely high modulation image for sub-32nm resolution.

Figure 16 is a plot of the information content of various systems: an i-line stepper, a 248nm stepper, a 248nm scanner, a 193nm scanner, an EUV scanner, 193nm with sidewall-spacer double pattering (SSDP), and interferometric systems with and without SSDP. In each case, the field size is assumed fixed except for the stepped square to scanned slot transition and k_1 trends downward from a value of 0.45 for i-line to 0.30 for 193nm and 0.25 for IL. A k_1 value of 0.7 is assumed for EUV. The information content (I) as the optical invariant is calculated for each case and values are identified on the plots for 32nm, 22nm, and 16nm half-pitch (hp) generations. As the 32nm generation is considered, it is seen that the 193nm projection lithography (possible only with high index materials) has an I value on par with EUV but significantly greater than 193nm SSDP. This would be expected and offers some validation regarding why the industry is moving in this direction. As 22nm hp is considered, 193nm projection lithography can no longer deliver but with SSDP, the I value is less than 3×10^4 while EUV increases to a values near 1.3×10^5. The comparison to SSDP does need to include any trim operation that would be added in the DP process, which would increase the I value. Both 32nm IL and IL SSDP have much lower I values, as does IL SSDP for 22nm hp. As 16nm hp is considered, there are just two contenders, EUV and IL SSDP. The I value for IL SSP is near 4.5×10^3 and EUV is near 1.8×10^5, assuming a constant k_1 value. If process and illumination improvements can reduce the EUV k_1 factor to values closer to 0.5, the I value could be reduced to 1.4×10^5. If the worst case scenario is considered for IL SSDP, it would require two IL steps and two trim steps. Using a current "N" generation 1.35NA 193nm immersion scanner, the composite I value become $2 \times (0.45 \times 10^4) + 2(6.5 \times 10^4) = 1.39 \times 10^5$. If an "N-1" generation scanner NA could be used, this value would be reduced accordingly, possibly to a value below 1.0×10^5. Further reduction is possible as the number of exposure steps can be reduced.

This analysis is for the information content of various technologies, which would need to be evaluated with regards to throughput to determine data rates. This can be done by using current or projected exposure times based on source power, system throughput, and photoresist sensitivities.

Downloaded from SPIE Digital Library on 27 Jan 2010 to 129.21.240.32. Terms of Use: http://spiedl.org/terms

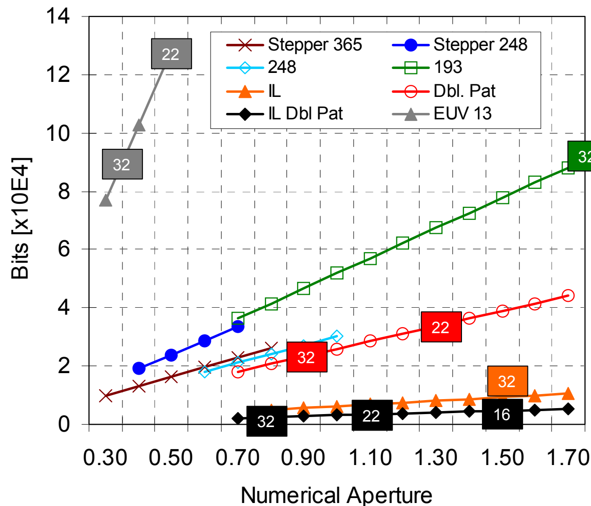

Figure 15. A plot of the information content (I) vs. numerical aperture for various lithography systems, together with the requirements for the 32nm, 22nm, and 16nm half pitch technology generations.

4.0 CONCLUSIONS

Many innovative, unconventional nanopatterning techniques are underway. Most of these technologies are useful for research and development in fields of nanotechnology. Other non-optical nanopatterning techniques exist as well including patterning based on natural force and adhesion and patterning with electrolytes and gels. For the most part, these approaches cannot resolve beyond the resolution of projection optical lithography. Some near field technologies, including the use of metamaterials, solid-fluid immersion, and coupled diffracted evanescent waves, could be employed to specific far-field planes in a projection lithography system. As sub-32nm hp technology is explored, interferometric lithography will become difficult to ignore. Especially when compared to other choices using simple metrics such as information content, where IL and IL combined with double pattering may dominate.

5.0 REFERENCES

[1] G. Reynolds, J. DeVelis, G. Parrent, B. Thompson, The New Physical Optics Notebook: Tutorials in Fourier Optics, SPIE Press (1989).
[2] F. De Martini, P. Ristori, E. Santamato, A.C.A. Zammit, Phys. Rev., B23, 3797 (1981).
[3] W. Srituravanich, N. Fang, C. Sun, Q. Luo, Z. Zhang, Nano Lett., 4, 1085-1088 (2004).
[4] W. Srituravanich, L. Pan, Y. Wang, C. Sun, D.B. Bogy, Z. Zhang, Nature NanoTech, 12 October 2008,1 (2008).
[5] B.W. Smith, Y. Fan, J. Zhou, N.Lafferty, A.Estroff, Proc. SPIE Optical Microlithography XIX, 6154, (2006).
[6] H.J. Lezec, T. Thio, Optics Express, 12(16), 3629-3651, (2004).
[7] N. Lafferty, A. Bourov, A. Estroff, B.W. Smith, RIT, J. Vac. Sci. Technol. B 26(6), 2192 (2008).
[8] N. Fang, H. Lee, C. Sun, X. Zhang, Science 22, Vol. 308(5721), (2005).
[9] B. Griffing, P. West, IEEE Elect. Dev . Lett., 4(1), 14- 16, (1983).
[10] S.W. Hell, J. Wichman, Opt. Lett. 19 (1994).
[11] S.W. Hell, M. Kroug, Appl. Phy. B 60 (1995).
[12] S.W. Hell, Phys. Lett A 326 (2004).
[13] B. W. Smith, Y. Fan, M. Slocum, L. Zavyalova, Proc. SPIE Optical Microlithography, vol. 5754, 2005.
[14] B. Tyrell, M. Fritze, D. Astolfi, R. Mallen, B. Wheeler, P. Rhyins, P. Martin, J. , J. Micro/Nanolith. , MEMS, and MOEMS, 1(3), 243 (2002).

Downloaded from SPIE Digital Library on 27 Jan 2010 to 129.21.240.32. Terms of Use: http://spiedl.org/terms